

1
2
3
4
5
6
7
8
9
10
11

Influence of a Dual Axis IoT- Based Off-Grid Solar Tracking System and Wheatstone Bridge on Efficient Energy Harvesting and Management

ABSTRACT

Addressing the increasing need for sustainable energy solutions, this study presents an advanced dual-axis solar tracking system tailored for Mirpur, Dhaka, Bangladesh (23.8123° N, 90.3740° E). By integrating Internet of Things (IoT) based intelligent power management and automated panel cleaning, we aim to optimize the efficiency of solar photovoltaic (PV) systems. Our design significantly outperforms traditional fixed PV setups, achieving an average voltage improvement of about 18.59% throughout the day. Real-time data monitoring showcases the system's adaptability, with Solar Voltage (SV) and Solar Current (SC) standard deviations recorded at 1.059 and 0.058, respectively. This system not only captures sunlight more efficiently but also ensures self-maintenance, reducing manual intervention. The integration of IoT capabilities provides real-time feedback and adaptability. With a small household size of 4-6 members and a basic electricity demand as a prototype version, the study reveals promising results for sustainable energy solutions. In future integrating a Microgrid system for improved energy distribution and storage, alongside implementing a smart fuzzy logic-based tracking system to optimize solar panel orientation for maximum power generation.

12
13
14
15
16
17
18
19
20
21
22
23
24
25
26

Keywords: Dual Axis, Solar Tracking, Panel Cleaning, Smart Power Management.

1. INTRODUCTION

The rising carbon footprint and global warming are direct consequences of the increased reliance on fossil fuels for power generation [1]. To mitigate these negative impacts, renewable energy has emerged as a pivotal long-term solution [2]. Among renewable sources, solar energy stands out due to its affordability, off-grid functionality, and minimal maintenance costs [3]. However, to maximize the output of solar photovoltaic (PV) systems, efficient utilization of solar energy is imperative [4]. This necessitates the implementation of intelligent solar systems capable of optimizing electricity utilization and maintaining system efficiency through preventive measures against heat and grime accumulation on PV panels [5].

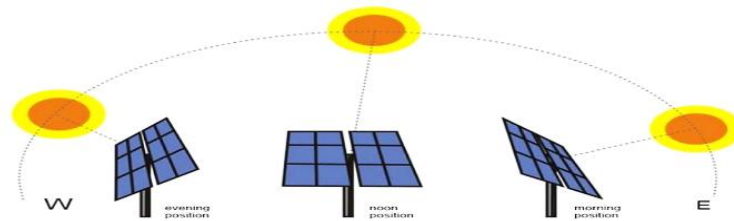
27
28
29
30
31
32

In recent years, there has been a notable surge in research efforts aimed at enhancing solar tracking systems, particularly through the integration of Internet of Things (IoT) technologies [6]. These advancements are designed to bolster the productivity and efficiency of solar panels by dynamically adjusting their orientation based on prevailing environmental conditions [7]. Such systems, equipped with IoT technology and intelligent features, leverage sensors, actuators, and IoT capabilities to enhance the energy efficiency of solar power

33 systems [8]. Notably, extensive testing has demonstrated significant energy production
34 improvements, up to 28.3%, compared to traditional fixed-mount systems, underscoring their
35 potential to advance renewable energy utilization significantly [9].

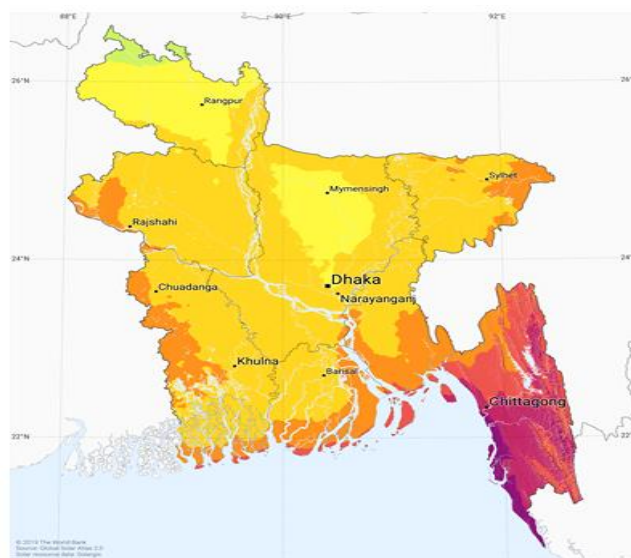
36 Further advancements include the incorporation of analog controllers and maximum power
37 point tracking (MPPT) devices, both integrated with IoT technology, to facilitate immediate
38 monitoring and control of solar power generation and battery charging [10]. Additionally,
39 emerging solar tracking systems powered by IoT, and machine learning algorithms offer
40 dynamic angle adjustments based on real-time data analysis, coupled with remote
41 monitoring and control capabilities for enhanced flexibility and ease of use [11]. Moreover,
42 the integration of IoT and Raspberry Pi technology has yielded cost-effective and adaptable
43 solar tracking systems suitable for various applications, including residential and small-scale
44 business environments [12].

45 Eventually, dual-axis solar tracking systems, bolstered by IoT technology, represent a
46 promising avenue for optimizing solar energy harvesting [13]. Through remote monitoring
47 and feedback control mechanisms, these systems effectively position solar panels relative to
48 sunlight, resulting in substantial improvements in energy collection efficiency compared to
49 fixed-tilt panels [14]. By implementing power management strategies, energy consumption
50 can be further minimized, highlighting the potential of these systems to enhance
51 sustainability and efficiency in solar energy utilization [15].
52



53
54
55

Fig. 1. Dual-axis solar tracking system [16]



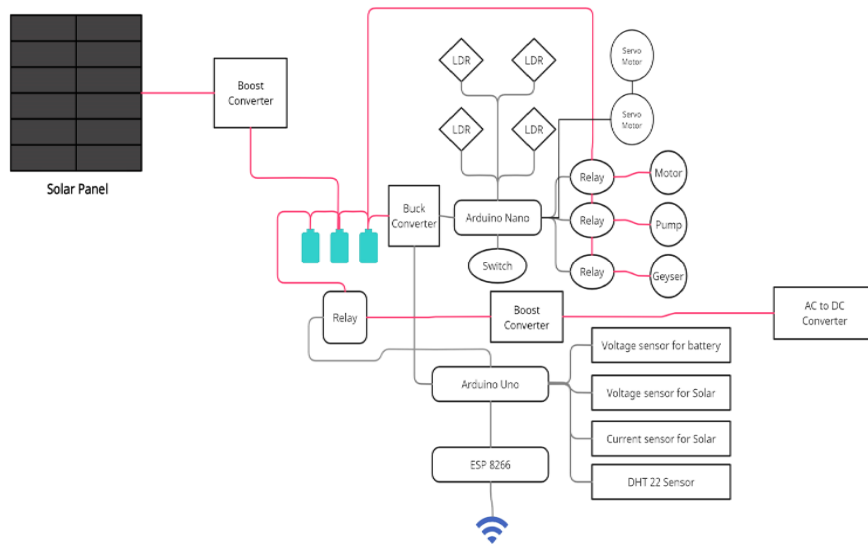
56
57
58

Fig. 2. Solar irradiance area of Bangladesh and Project test location [17]

59 We propose a system with automatic panel cleaning and solar tracking to maximize energy
60 harvesting potential. We also use Internet of Things (IoT) gadgets to track and report data
61 like solar energy output, battery life, and ambient temperature from a central location. The
62 electricity demand is expected to continue rising globally, particularly in the post-COVID era,
63 as reported by the International Energy Agency (IEA) [18].

64 2. METHODOLOGY

65



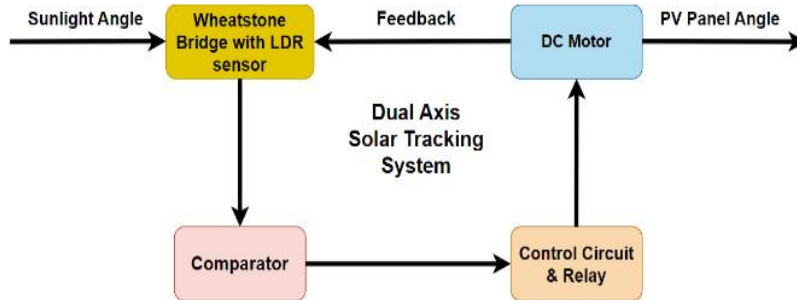
66
67
68

Fig. 3. System Structure Block Diagram

69 The block diagram of the system structure (Fig. 3) depicts the system's overall operation.
70 The system includes a solar panel that generates the essential energy for the system to
71 function. The integration of a boost converter plays a pivotal role in enhancing the system's
72 efficiency by transforming a lower voltage into a higher one. Complementing this, a 14.8-volt
73 Lithium-ion battery is seamlessly integrated to store and supply energy to the system. This
74 setup necessitates the incorporation of two boost converters within the design: one
75 dedicated to elevating the solar panel's voltage to 16.8 volts and the other aimed at
76 increasing the 12-volt AC to DC converter's voltage to the same level. This synchronization
77 ensures optimal performance, particularly when the battery pack attains its maximum charge
78 of 16.8 volts. Additionally, the initial utilization of the Wheatstone Bridge serves to measure
79 shallow resistance values with precision, operating through voltage division. Its pivotal
80 application lies in measuring variations in sensor resistance, providing a robust foundation
81 for system calibration and optimization [19].

82 The implementation of the Dual Axis Solar Tracking control system represents a significant
83 stride towards system robustness and efficiency. This closed-loop system seamlessly
84 integrates the utilization of a Wheatstone bridge circuit and light-dependent resistors (LDRs),
85 forming the backbone of the tracking mechanism. A compact and purpose-built control
86 system is meticulously developed and assembled to validate the proposed approach,
87 ensuring its effectiveness and efficiency. Within this framework, the reference input signal in
88 the closed-loop dual-axis solar system is intricately tied to sunlight intensity, as depicted in
89 Fig 4. To enable seamless solar tracking, the integration of optical sensors becomes
90 imperative to accurately discern the sun's position. Leveraging these optical sensors, the

91 proposed tracking system dynamically adjusts the photovoltaic (PV) panel in alignment with
92 the sun's angle, optimizing energy harvesting and system performance.



93

94

Fig. 4. Dual Axis Solar System Block Diagram

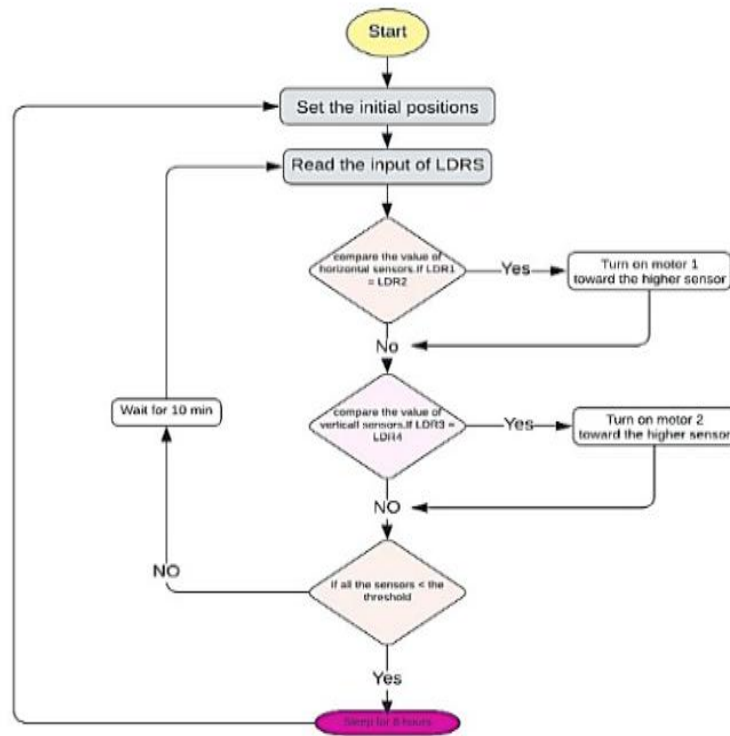
95 As light intensity increases, LDR sensors' electrical resistance decreases. A voltage
96 differential emerges from an LDR sensor-generated voltage imbalance in the Wheatstone
97 bridge branches. Figure 2 shows the difference between solar radiation angle and PV panel
98 position. The Wheatstone bridge output voltage is then boosted by the operational amplifiers
99 (op-amps). Control circuits trigger the relay using operational amplifier output voltage. The
100 relay starts engine rotation in the tracking system to move it in the right direction. Under ST
101 control, the PV panel will rotate on its axis. This automatic mechanism positions the PV
102 panel at the proper angle to the sun [20]. This process continues until the voltage disparity in
103 the bridge branches decreases below a predetermined threshold value.

104 A Buck converter is used to supply 5 volts to the microcontroller and servo actuator. Two
105 boost converters are required because the solar panel's voltage output is unstable and
106 dependent on several variables, such as the intensity of sunlight, temperature, and shading
107 effects. Three microcontrollers, Arduino NANO, Arduino Uno, and ESP 8266 are incorporated
108 into the system's design. Arduino NANO controls dual-axis solar tracking systems, cleans
109 solar panels, and operates geyser systems. The LDR sensor determines the movement of
110 the servo motor, and the cleaning motor and pump are activated at predetermined intervals.
111 In addition, the geyser system can be controlled via a valve. Arduino Uno is outfitted with two
112 voltage sensors, a current sensor, and a DHT 22 sensor (consisting of a humidity sensor
113 and a thermistor to measure air and generate digital data directly). The detected data is then
114 transmitted via serial communication to ESP 8266. The data is sent to the web server by
115 ESP 8266.

116 2.1 Dual Axis Solar Panel Movement Flowchart

117 Fig. 5 represents the Dual Axis Solar Panel Movement flowchart depicts the sequence of
118 actions to be carried out by the command. The program begins with the power to commence
119 and then directs the solar panel to its initial position. It accumulates and processes all the
120 LDR sensor inputs. The program contrasts the values of the horizontal sensor data, namely
121 whether LDR1 and LDR2 are equivalent. If the result is positive, Motor1 will be commanded
122 to move towards the sensor above it. However, if the impact is negative, the program
123 immediately compares the values of vertical LDR sensors. It determines whether LDR3 is

124 equal to LDR4. If the result is positive, it instructs Motor2 to move towards the higher-up
125 sensor.
126



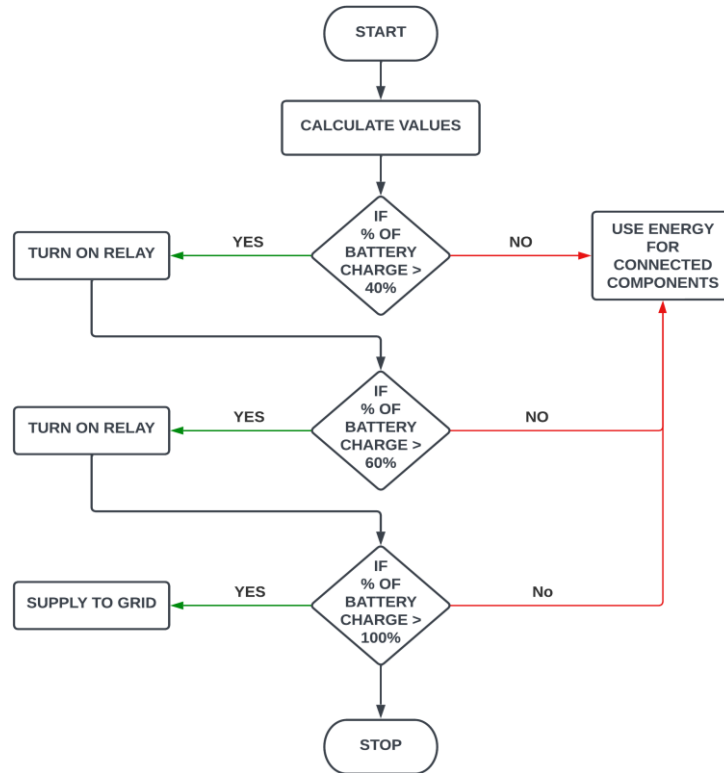
127
128
129

Fig. 5. Dual-axis solar panel movement flowchart

130 If the result is negative, the program then determines whether all sensor values are below
131 the threshold value. If the result is negative, the program delays ten minutes before
132 rereading the LDR sensor values. If the result is positive, the program sleeps for six hours
133 and restarts the procedure by repositioning the solar panel.

134
135

2.2Power System Flow Diagram



136
137
138

Fig. 6. Power management system flowchart

139 Fig. 6 depicts a comprehensive overview of the sequential steps the power management
140 system follows in response to user commands. The flowchart begins with the "start"
141 command and continues with the battery's charge percentage calculation. If it is determined
142 that the battery charge is 40%, the system will command the relay to power on. An alarm will
143 sound if the battery charge declines below 40%. The system will also control the relay to pull
144 on when the battery charge reaches 60%. When the battery reaches its maximum capacity,
145 the system will command the excess generating current to be supplied to the grid.

146
147
148

3. DESIGN AND SIMULATION

149 SolidWorks, a popular CAD software, was used to construct an elaborate 3D model of the
150 project in Fig 7. The 3D model correctly depicts the project concept and demonstrates the
151 anticipated conclusion. System-critical solar panels are on top of the model. LDR (light-



152 dependent resistor) sensors on the top and a gear motor on the left ensure precise solar
153 panel cleaner control. Two strategically placed servo motors for horizontal and vertical
154 movements enable dual-axis rotation for better tracking. For precise and smooth motor
155 positioning, a well-designed frame is needed. A hardware component box holds vital system
156 components and is delicately attached to the frame. The model's bottom battery ensures
157 power supply, maximizing space utilization and system performance.

158
159
160

Fig. 7.



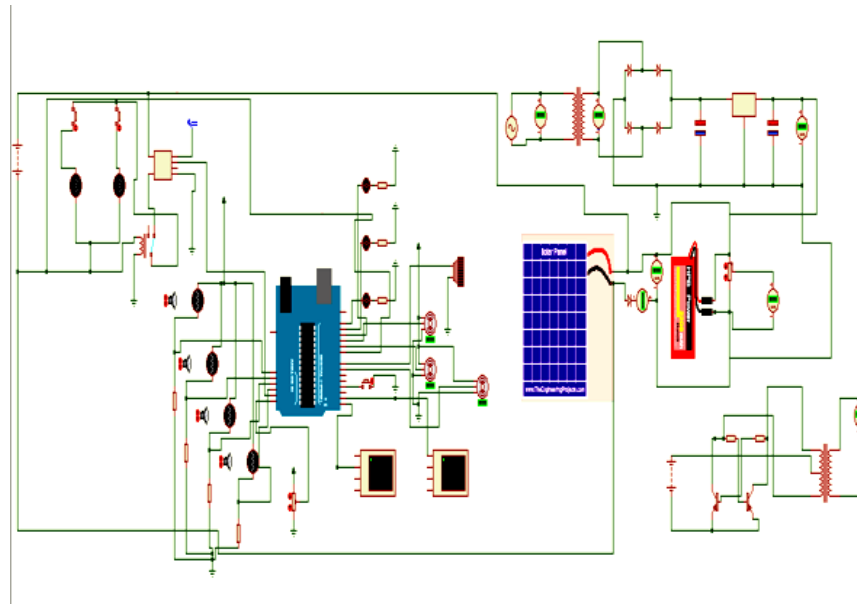
163 Fig. 8.
164 the
165 power
166 lets

171 varied

Prototype 3D model of the project.

3.1 Simulation of Robotic System and Operation

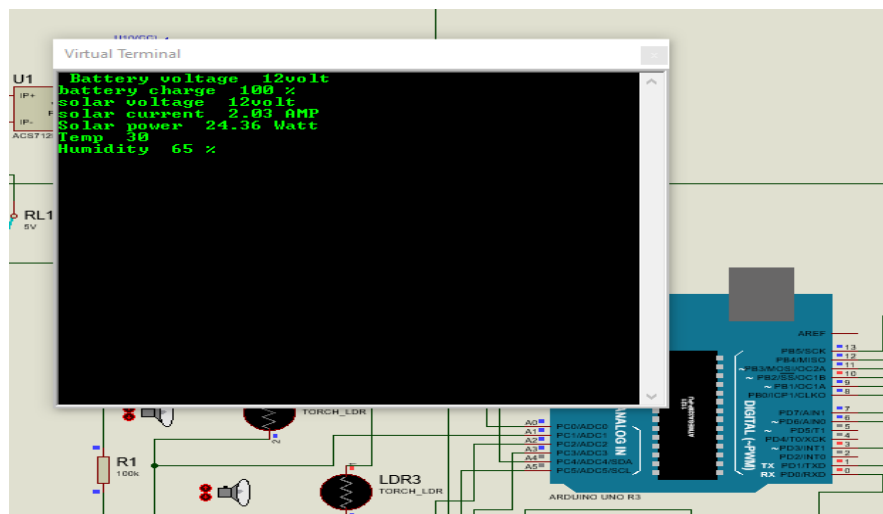
displays the Simulation models assessing IoT-based intelligent photovoltaic solar system's performance before construction. It you test multiple design configurations and operating parameters and predict system performance. Simulation models can estimate a solar power system's energy output, battery charge, and efficiency in weather conditions.



172
173
174

Fig. 8. Micro-controller-based Power controller system designed in Proteus.

175 The simulation of the robotic system and its operations was carried out with the help of the
176 Proteus program. Fig. 9 shows that an Arduino Uno R3 microcontroller served as the
177 simulation's primary processing unit, and its use was facilitated by incorporating this
178 component into its design. Within the simulation, there were a total of four LDR sensors
179 used. In addition, the simulation was equipped with three servo motors, which stood in for
180 the cleaning brush motor, the horizontal axis motor, and the vertical axis motor, respectively.
181 Additionally, to raise the voltage of both the solar panels and the 12-volt AC to DC converter,
182 the system was equipped with two boost converters. The objective of these converters was
183 to enhance the voltage. In addition, a buck converter was developed to supply energy to the
184 microcontroller and the servo motor at a voltage of 5 volts. In the final step of the simulation,
185 an energy storage device comprised of a solar panel and a battery was used.



186
187
188

Fig. 9. Simulation result of micro-controller-based power controller system

189 **4. IMPLEMENTATION & RESULT**

190

191 Fig. 10 depicts the final prototype of a project that includes a dual-axis solar tracking system,
192 a panel cleaning system, and a power management system. Previously, a 3D model of the
193 project was presented, and now its completion has been accomplished. The final product is
194 a solar panel that converts sunlight into electricity. On the upper portion of the meeting, there
195 are LDR sensors, and on the right side, there is a cleaner gear motor to move the cleaning
196 brush across the solar panel. A horizontal servo motor is located beneath the board and is
197 responsible for horizontal panel movement. The buck converter and vertical servo motor,
198 which move the panel along the vertical axis, are located beneath this. This results in a dual
199 axis tracking system for the project, enabling the solar panel to be moved along both the
200 horizontal and vertical dimensions.
201

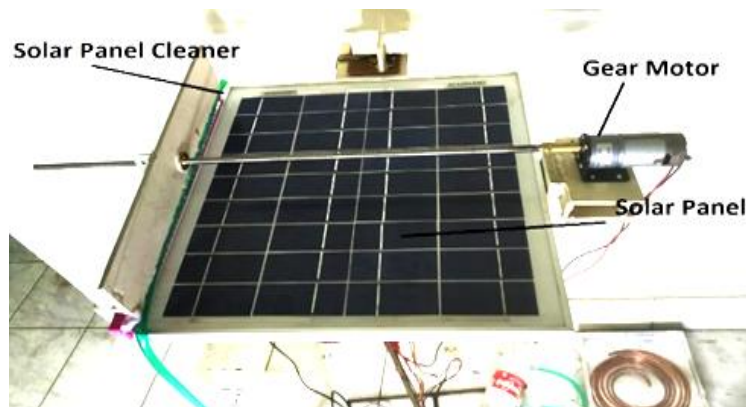


202

203

204 **Fig. 10. Implemented dual-axis solar tracking, panel cleaning, and power management**
205 **system project.**

206 Fig. 11 depicts a top view of the project, displaying the solar panel, LDR sensors, cleaner,
207 and cleaner gear motor. The solar panel and LDR sensors work together as a tracking
208 system component, whereas the cleaner and cleaner motor facilitate the solar panel
209 cleaning system.



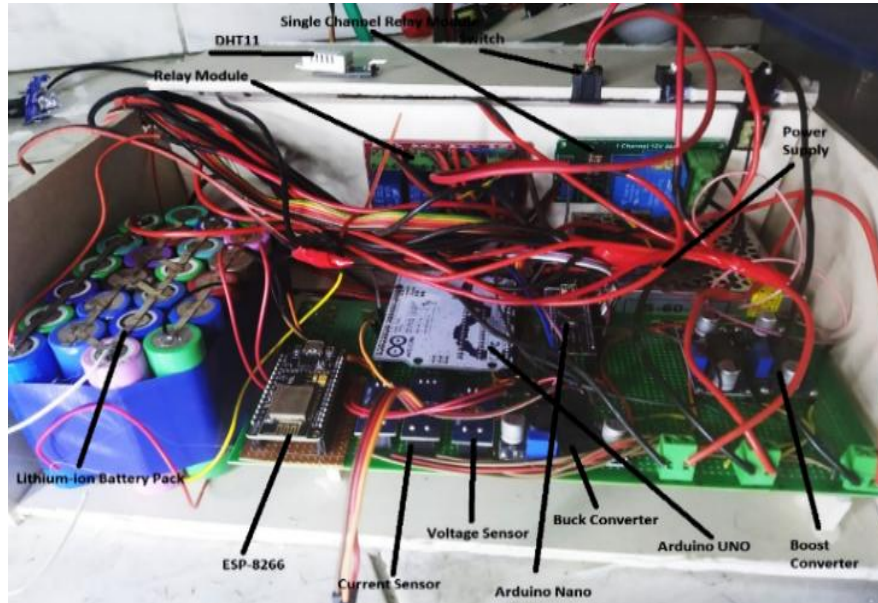
210

211

212

Fig. 11. Top view of solar sun tracking and cleaning system.

213 Fig. 11 depicts the sun monitoring and dual-axis movement systems incorporated into the
214 project. The primary function of the dual-axis movement system is to allow the solar panel to
215 move horizontally and vertically. This is accomplished by employing a horizontal servo motor
216 to facilitate movement in the horizontal plane and a vertical servo motor to boost the solar
217 panel about its vertical axis. In addition, a buck converter is integrated into the system to
218 provide 5 volts of stable power to the microcontroller and servo actuator.
219



220
221
222

Fig. 12. Inside of hardware primary device

223 Fig. 12 depicts the project's primary terminal unit for power and control. This image
224 represents all of the project's constituent parts. The Arduino Uno, Arduino Nano, and ESP
225 8266 are readily identifiable as the project's primary processing devices. Additionally, the
226 image displays the Boost and Buck converters. The lithium-ion battery cell is positioned on
227 the image's left side. In addition, the painting depicts one current sensor and one voltage
228 sensor used for measuring purposes. The image's reverse side displays the motor control
229 and single-channel relay modules. In addition, DHT11 and the switch are located adjacent to
230 these modules.

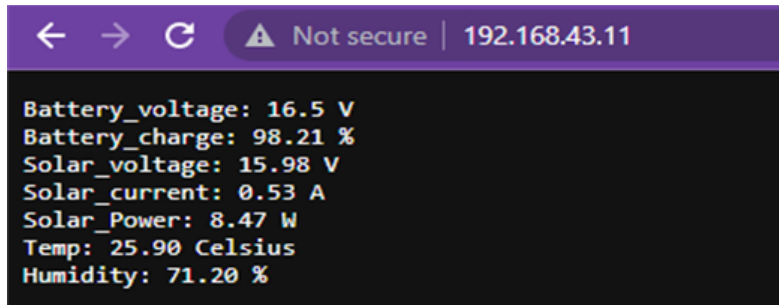
231 The simulation result is seen in this photo, which depicts the virtual terminal. It displays the
232 voltage of the battery, as well as the battery's percentage of charge, and the voltage,
233 current, and power of the solar panel. The system draws power from the grid if the battery
234 charge is lower than 40 percent, equivalent to 4.2 volts. Let's say that the battery has 4 volts.
235 The battery pack operates at 16.8 volts. The calculation is:

236

$$= ((4*100)/16.8) \% = 23.81\%$$

237
238

In this situation, this system takes power from the grid.



239
240
241

Fig. 13. Hardware result of the Project in a Web-based interface.

242 Fig. 13 displays the outcome of the implemented gadget. <https://192.168.43.11> is the
243 Internet Protocol address of the data display website.

244 **Table 1. The Percentage Improvement in Voltage for The Dual Axis Setup Over the**
245 **Fixed PV Setup**
246

Time (Hour)	Fixed PV Setup (V)	Dual Axis Setup (V)	Improvement Voltage (%)
06.00 AM	8.89	10.14	14.06
07.00 AM	10.25	12.57	22.63
08.00 AM	12.31	14.33	16.41
09.00 AM	13.36	14.69	9.96
10.00 AM	13.89	15.11	8.78
11.00 AM	14.02	15.34	9.42
12.01 PM (at Noon)	15.13	15.98	5.62
01.00 PM	14.46	15.66	8.30
02.00 PM	13.67	15.25	11.56
03.00 PM	12.49	14.82	18.65
04.00 PM	10.92	14.16	29.67
05.00 PM	9.14	13.63	49.12

247
248
249
250
251
252
253

In Table 1, the average percentage improvement over the day is approximately 18.59%. This means, on average, the Dual Axis Setup provides an 18.59% improvement in voltage over the Fixed PV Setup throughout the day. This result shows that the Dual Axis Setup is significantly more efficient than the fixed PV Setup, as it consistently produces higher voltage outputs across all times of the day.

254
255
256
257
258
259

Table 2 shows the hardware findings from a monitoring day from 6:00 AM to 6:00 PM. Battery voltage, battery charge, solar voltage, solar current, solar power, temperature, and humidity are all included in the findings. Where, Temperature, humidity, light intensity, and electricity output from solar panels are all displayed. Short forms used in the table are Battery Voltage = BV, Battery charge = BC, Solar Voltage= SV, Solar Current = SC, Solar power = SP, Temperature = Temp, Humidity = Hum.

260
261
262

Table 2. Implemented Hardware Result

Time	BV	BC	SV	SC	SP	Temp	Hum
6 AM	15.3	90.54 %	10.14	0.13	0.91	23.2	70.88
7 AM	15.4	91.28 %	12.57	0.14	0.95	23.9	70.96
8 AM	15.5	92.26 %	14.33	0.14	0.98	24.8	71.07
9 AM	15.6	92.85 %	14.69	0.14	1.2	25.0	71.02

10 AM	15.7	93.45 %	15.11	0.16	1.45	25.0	71.30
11 AM	15.9	94.65 %	15.34	0.19	1.99	27.20	72.05
12 PM (at Noon)	16.0	95.23 %	15.87	0.19	2.08	27.46	72.43
1 PM	16.2	96.4 %	15.66	0.21	2.74	27.40	72.44
2 PM	16.5	98.21 %	15.25	0.35	6.25	28.05	71.03
3 PM	16.8	100 %	14.82	0.25	4.12	26.01	71.67
4 PM	16.8	100 %	14.16	0.27	4.18	24.47	70.04
5 PM	16.8	100 %	13.63	0.30	5.07	23.41	70.38
6 PM	16.8	100 %	11.91	0.21	3.42	23.19	70.18

263

264

265

266

267

268

269

270

271

272

273

274

275

The solar voltage (SV) rises from 6 AM, peaks around midday, and then diminishes, aligning with anticipated solar intensity patterns. The consistent SV curve indicates the system's efficient adaptability to sunlight variations. Similarly, the solar current (SC) follows this trend but has a distinct surge at 2 PM, possibly due to unique environmental circumstances. Solar power (SP), being the result of voltage and current, mirrors these trends, with a marked spike at 2 PM, signaling a notable boost in energy production. In essence, the steady SV and SC trends highlight the system's effective response to daily solar changes, proving the Dual Axis Setup's capability in optimal solar tracking and energy harnessing. The standard deviations for rate changes in Solar Voltage (SV) and Solar Current (SC) are 1.059 and 0.058, respectively. The SC low value indicates a smoother and more consistent response to daily solar variations. Both values suggest the system effectively adapts to changing solar conditions [21].

276

5. CONCLUSION

277

278

279

280

281

282

283

284

285

286

287

In this study, we successfully engineered a dual-axis solar tracking system, realizing an average voltage improvement of approximately 18.59% over traditional fixed PV setups. Our system's incorporation of an automated cleaning mechanism and IoT capabilities ensured real-time monitoring and adaptability, as evidenced by the Solar Voltage (SV) and Solar Current (SC) standard deviations of 1.059 and 0.058, respectively. Future directions include integrating AI for optimal panel orientations, fortifying IoT security, exploring advanced battery storage solutions, enhancing system scalability, and merging with other renewable energy sources. This endeavor represents a significant leap in sustainable solar energy solutions, promising broader applications in the future.

288

REFERENCES

289

290

291

292

293

[1] Strielkowski, Wadim, Lubomír Cívín, Elena Tarkhanova, Manuela Tvaronavičienė, and Yelena Petrenko. 2021. "Renewable Energy in the Sustainable Development of Electrical Power Sector: A Review" *Energies* 14, no. 24: 8240. <https://doi.org/10.3390/en14248240>.

294

295

[2] A.R. Amelia et al 2020 IOP Conf. Ser.: Mater. Sci. Eng. 767 012052 DOI 10.1088/1757-899X/767/1/012052.

296

297

298

[3] P. Muthukumar, S. Manikandan, R. Muniraj, T. Jarin, Ann Sebi, Energy efficient dual axis solar tracking system using IOT, Measurement: Sensors, Volume 28, 2023, 100825, ISSN 2665-9174, <https://doi.org/10.1016/j.measen.2023.100825>.

- 299 [4] Rokonzaman, Md., Mohammad Shakeri, Fazrena Azlee Hamid, Mahmuda Khatun
300 Mishu, Jagadeesh Pasupuleti, Kazi Sajedur Rahman, Sieh Kiong Tiong, and Nowshad Amin.
301 2020. "IoT-Enabled High Efficiency Smart Solar Charge Controller with Maximum Power
302 Point Tracking—Design, Hardware Implementation and Performance Testing" *Electronics* 9,
303 no. 8: 1267. <https://doi.org/10.3390/electronics9081267>.
- 304 [5] M. Saeedi and R. Effatnejad, "A New Design of Dual-Axis Solar Tracking System
305 with LDR Sensors by Using the Wheatstone Bridge Circuit," in *IEEE Sensors Journal*, vol.
306 21, no. 13, pp. 14915-14922, 1 July1, 2021, doi: 10.1109/JSEN.2021.3072876.
- 307 [6] A Suryanto et al 2021 IOP Conf. Ser.: Earth Environ. Sci. 700 012016 DOI
308 10.1088/1755-1315/700/1/012016.
- 309 [7] Sandhiya, B., Raja, S., Raja, R., Ethiraj, M. and Rasool, M.I., 2024, January. Internet
310 of things based dual axis solar tracking system. In *AIP Conference Proceedings* (Vol. 2802,
311 No. 1). AIP Publishing.
- 312 [8] Udit Mamodiya, Neeraj Tiwari, Dual-axis solar tracking system with different control
313 strategies for improved energy efficiency, *Computers and Electrical Engineering*, Volume 111,
314 Part A, 2023, 108920, ISSN 0045-7906, <https://doi.org/10.1016/j.compeleceng.2023.108920>.
- 315 [9] P. Muthukumar, S. Manikandan, R. Muniraj, T. Jarin, Ann Sebi, Energy efficient dual
316 axis solar tracking system using IOT, *Measurement: Sensors*, Volume 28, 2023, 100825, ISSN
317 2665-9174, <https://doi.org/10.1016/j.measen.2023.100825>.
- 318 [10] Kim, Gi Yong, Doo Sol Han, and Zoonky Lee. 2020. "Solar Panel Tilt Angle
319 Optimization Using Machine Learning Model: A Case Study of Daegu City, South Korea"
320 *Energies* 13, no. 3: 529. <https://doi.org/10.3390/en13030529>.
- 321 [11] El Hammoumi, A., Motahhir, S., El Ghzizal, A., Derouich, A. (2021). Internet of
322 Things-Based Solar Tracker System. In: Motahhir, S., Eltamaly, A.M. (eds) *Advanced
323 Technologies for Solar Photovoltaics Energy Systems*. Green Energy and Technology.
324 Springer, Cham. https://doi.org/10.1007/978-3-030-64565-6_4.
- 325 [12] Timothy Laseinde, Dominic Ramere, Low-cost automatic multi-axis solar tracking
326 system for performance improvement in vertical support solar panels using Arduino board,
327 *International Journal of Low-Carbon Technologies*, Volume 14, Issue 1, March 2019, Pages
328 76–82, <https://doi.org/10.1093/ijlct/cty058>.
- 329 [13] Barbón, A. & Fernández-Rubiera, J.A. & Martínez-Valledor, L. & Pérez-Fernández,
330 A. & Bayón, L., 2021. "Design and construction of a solar tracking system for small-scale
331 linear Fresnel reflector with three movements," *Applied Energy*, Elsevier, vol. 285(C).
- 332 [14] Thungsuk, Nuttee, Thaweesak Tanaram, Arckarakit Chaitanakulwat,
333 Teerawut Savangboon, Apidat Songruk, Narong Mungkung, Theerapong Maneepen, Somchai
334 Arunrungrusmi, Wittawat Poonthong, Nat Kasayapanand, and et al. 2023. "Performance
335 Analysis of Solar Tracking Systems by Five-Position Angles with a Single Axis and Dual
336 Axis" *Energies* 16, no. 16: 5869. <https://doi.org/10.3390/en16165869>.
- 337 [15] Brahmaiah, V. Siva and B, Mr. Rajkiran and Sharma, Pradeep, An Intellectual Dual
338 Axis Efficient Solar Tracking System by Using IoT Integrated Controller (February 21, 2020).
339 *Proceedings of the 4th International Conference: Innovative Advancement in Engineering &*

- 340 Technology (IAET) 2020, Available at SSRN: <https://ssrn.com/abstract=3554005> or
341 <http://dx.doi.org/10.2139/ssrn.3554005>.
- 342 [16] Mohamed, Elhamy & Adel, M & Gamal, A & Rashad, Sonya & Hamdy, Alaa &
343 Hashem, Essam. (2016). Design and Implementation of Sun Tracking System.
- 344 [17] Mojumder, M.H., Hasanuzzaman, M. & Cuce, E. Prospects and challenges of
345 renewable energy-based microgrid system in Bangladesh: a comprehensive review. *Clean*
346 *Techn Environ Policy* 24, 1987–2009 (2022). <https://doi.org/10.1007/s10098-022-02301-5>.
- 347 [18] International Energy Agency, "Electricity market report 2020," Jul. 2020. [Online].
348 Available: <https://www.iea.org/reports/electricity-market-report-2020>. [Accessed: Apr. 29,
349 2023].
- 350 [19] P. R. Nagarajan, B. George, and V. J. Kumar, "A Linearizing Digitizer for
351 Wheatstone Bridge Based Signal Conditioning of Resistive Sensors," *IEEE Sensors Journal*,
352 vol. 17, no. 6, pp. 1696–1705, Mar. 2017.
- 353 [20] J.-M. Wang and C.-L. Lu, "Design and Implementation of a Sun Tracker with a Dual-
354 Axis Single Motor for an Optical Sensor-Based Photovoltaic System," *Sensors*, vol. 13, no.
355 3, pp. 3157–3168, Mar. 2013.
- 356 [21] G. Cibira and M. Koščová, "Photovoltaic module parameters acquisition model,"
357 *Applied Surface Science*, vol. 312, pp. 74–80, Sep. 2014, doi:
358 <https://doi.org/10.1016/j.apsusc.2014.05.080>.